

ADMM-Based Channel Estimation Methods for Millimeter Wave MIMO System

Prateek Saurabh Srivastav
Department of Information and Communication
Engineering,
Pukyong National University,
Busan, South Korea
Email: psrivastav.619@gmail.com

Hoon Lee
Department of Information and Communication
Engineering,
Pukyong National University,
Busan, South Korea
Email: hlee@pknu.ac.kr

Abstract— Millimeter wave (mmWave) communication techniques have been regarded as promising solutions for wireless communication networks. However, short wavelength of mmWave signals poses fundamental challenges in estimating wireless channels. This paper tackles the channel estimation problems for frequency selective mmWave imposed on a multiple-input and multiple-output (MIMO) systems. In particular, we leverage the low-rank and sparse properties of mmWave channel matrices. The alternating direction method of multipliers (ADMM) with a relaxation parameter in a symmetrical order is employed. The numerical results exhibit the superiority of proposed methodology in terms of mean-squared-error and spectral efficiency.

Keywords—*Millimeter Wave, Channel Estimation, MIMO, ADMM.*

I. INTRODUCTION

Millimeter Wave (mmWave) is a possibility that might be considered for the next generations of wireless communications as it has an extremely high bandwidth. In spite of the fact that mmWave communication systems are subject to severe pathloss and atmospheric attenuation, the mmWave spectrum, because of its short wavelengths, has the ability to assemble multiple antennas into a single array. This is the fundamental concept behind high directional beamforming.

In the IEEE 802.11ad standard for single-stream communication, directional beamforming is used. Throughout this standard, a large number of antenna components are linked to a single radio frequency (RF) chain through an analog network of phase shifters or lenses. Together with hybrid beamforming (HBF), the 5G new radio (NR) technology [1] was able to accomplish the goal of delivering faster data speeds [2]. A maximum of four spatial streams are used under this operation. Analog and digital signal processing methods are used by HBF to link a substantial proportion of antenna segments to a small number of RF chains. To realize such a system, it is essential to acquire the prior knowledge of channel state information (CSI).

Nevertheless, due the vast number of transceiver antenna components and the high degree of unpredictability of the channel, this operation is one that is very difficult to carry out in reality [3]. In spite of this, several techniques for producing beamforming (BF) vectors that are appropriate for CSI estimation and that call for receiver feedback have been devised [4],[5]. Beam codebook systems that do not use receiver feedback have also been reported. Examples of these included the static dictionary computations or explicit beam training techniques, are explained in [6]–[10]. In most of the implementations, estimation procedure of CSI has been treated as a compressive sensing problem [11].

When it comes to reconstructing the sparse channel gain matrix, the orthogonal matching pursuit (OMP) algorithm [12] is a prominent greedy technique. Despite the fact that power leakage has been observed in beam dictionaries attributable to the discretization of arrival and departure angles, these methodologies for channel estimation have not been able to reach their full potential [7]. In [13]–[15] wireless channel sparsity and low rank characteristics have lately been used for effective CSI estimation. According to [13] and [16] channel estimation for narrowband mmWave MIMO using HBF transceivers may be accomplished using a two-stage technique. In [14], a matrix completion-based technique for a narrowband channel that utilizes low rank and sparsity together is described.

In this study, short training periods for frequency selective wideband mmWave massive MIMO systems with HBF structures are examined. At the receiver side, a multi-purpose optimization problem is constructed to estimate the CSI matrix using the low-rank property of the received signal matrix and the sparsity of the channel matrix. The proposed channel estimation technique is based on The alternating direction method of multipliers (ADMM) [17] with a relaxation factor in a symmetrical order.

The contributions of this paper are summarized as follows:

- A hybrid channel estimation approach with a relaxation factor is proposed for wideband mmWave MIMO system. An analogue combining architecture with a random sampling structure described in [18] is used to develop this channel estimation approach.
- For the case of multiple receiver reception (during the beam training), the rank of the wideband mmWave MIMO channel matrix is of the lower order. Therefore, the analogue portion of receivers will reflect the same rank as the wideband channel matrix does. The proposed method uses a nuclear norm to ensure low-rank channel matrix approximations and a l_1 norm to guarantee sparsity.

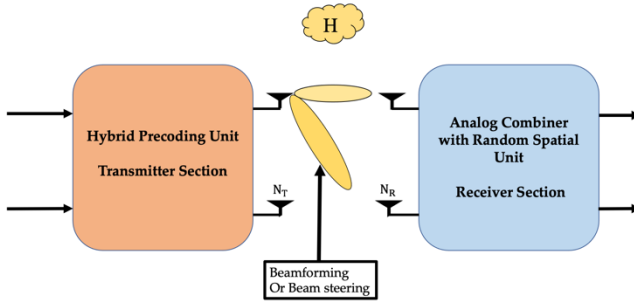


Fig. 1. Hybrid mmWave MIMO system with Analog Combiner and random spatial sampling unit.

II. SYSTEM MODEL

As shown in fig. 1, we consider a system with multi-antenna transmitter and receiver. Let N_T and N_R be the number of transmit and receive antennas, respectively. Frequency selective mmWave MIMO channel model described in [19] is considered for the detailed study. A frequency selective geometric virtual (GV) model is employed where the channel matrix millimeter-wave MIMO system, which includes a channel gain matrix $H(l) \in \mathbb{C}^{N_R \times N_T}$ of the l -th delay tap ($l = 0, 1, 2, \dots, L-1$), is expressed as,

$$H(l) \triangleq \sqrt{\frac{N_T N_R}{N_p}} \sum_{k=1}^{N_p} \alpha_k p(lT_s - \tau_k) a_R(\Phi_k) a_T^H(\theta_k), \quad (1)$$

Here, N_p is the number of propagation path for each channel delay tap. α_k denotes the complex channel gain following complex Gaussian distribution with zero mean and unit variance τ_k stands for the delay of the k -th path. $p(\tau_k)$ indicates the pulse shaping filter. $a_T^H(\theta_k) \in \mathbb{C}^{N_T}$ and $a_R(\Phi_k) \in \mathbb{C}^{N_R}$ represents the array response vectors at the transmitters and receivers, respectively.

As per the virtual beamspace representation model described in [20], $H(l)$ can be further written by,

$$H(l) = D_R Z(l) D_T^H, \quad (2)$$

Where, $D_R \in \mathbb{C}^{N_R \times N_R}$ and $D_T \in \mathbb{C}^{N_T \times N_T}$ account for the unitary discrete fourier transformation (DFT) matrices, respectively and $Z(l) \in \mathbb{C}^{N_R \times N_T}$ denotes the sparse DFT matrix which merely have the few virtual channel gains of higher amplitude and also determines the sparsity level of angular discretization.

On the basis of analog combining architecture following the random spatial sampling process, the wideband MIMO channel sounding procedure, the channel matrix described in eq (2) can be further rewritten as [18],

$$\tilde{Y} = D_R \bar{Z} (I_L \otimes D_T^H) \tilde{\psi}, \quad (3)$$

Where, $\tilde{Y} \in \mathbb{C}^{N_R \times T}$, $\tilde{\psi} \triangleq [\psi^T(0) \psi^T(1), \dots, \psi^T(L-1)] \in \mathbb{C}^{LN_T \times T}$ contains the training symbol, $\bar{Z} \triangleq [Z(0)Z(1), \dots, Z(L-1)] \in \mathbb{C}^{N_R \times LN_T}$, and I_L is an identity matrix of size $L \times L$.

The output R_Ω of the analog HBF combiner is obtained as,

$$R_\Omega \triangleq \Omega \circ (Y + N), \quad (4)$$

where, $Y = A \bar{Z} B$, $A \triangleq (W_{RF}^e)^H D_R \in \mathbb{C}^{M_R^e \times N_R}$, $B \triangleq (I_L \otimes D_T^H) \tilde{\psi} \in \mathbb{C}^{LN_T \times T}$, $N = (W_{RF}^e)^H (\tilde{N})$ is the additive white gaussian noise (AWGN) with independent and identically (I.I.D.) distributed with zero means and variance σ_n^2 . W_{RF}^e is the extended analog combiner with unit magnitude elements. The analog HBF structure performs sampling of M_R^e outputs of extended combiner W_{RF}^e by only considering M_R signals to the receive RF chains. $\tilde{N} \in \mathbb{C}^{N_R \times T}$ is the AWGN noise of analog HBF combiner. Matrix $\Omega \in \{0, 1\}^{N_R \times T}$ has TM_R ones and $T(N_R - M_R)$ zeros [18]. Every column of R_Ω have M_R non zero rows of N_T .

III. PROBLEM DESCRIPTION

As eq (4) demonstrates, by taking leverage of the low rank property of the training symbol's matrix Y and the sparse structure of Z the optimization problem can be formulated as follows,

$$\begin{aligned} & \min_{Y, \bar{Z}} \Gamma_Y \|Y\|_* + \Gamma_{\bar{Z}} \|\bar{Z}\|_1 \\ & \text{s.t. } R_\Omega \triangleq \Omega \circ (Y + N) \text{ and } Y = A \bar{Z} B \end{aligned} \quad (5)$$

Afterwards, two auxiliary matrices, $X \in \mathbb{C}^{N_R \times N_T}$ and $C \triangleq Y - A \bar{Z} B$, are introduced, then problem (5) can be recast to

$$\begin{aligned} & \min_{Y, \bar{Z}, X, C} \Gamma_Y \|Y\|_* + \Gamma_{\bar{Z}} \|\bar{Z}\|_1 + \frac{1}{2} \|C\|_F^2 + \frac{1}{2} \|\Omega \circ X - R_\Omega\|_F^2 \\ & \text{s.t.}, \quad Y = X \text{ and } C = Y - A \bar{Z} B \end{aligned} \quad (6)$$

The sum of the four variables that comprise the cost function is Y , \bar{Z} , X , and C . The discretization error is included in the third

term of the objective function, whereas the noise is involved as the fourth term of the objective function. In this scenario, the sum of a matrix's singular values is calculated using a nuclear norm. The nuclear norm is also the convex lower limit of any matrix, with the tightest convexity. Therefore, the nuclear norm is applied to attain matrix Y 's low rank characteristic. Alternatively, \bar{Z} is limited by the l_1 - *norm* to assure sparsity. In contrast, the weighting factors Γ_Y and $\Gamma_{\bar{Z}}$ are dependent on the number of propagation channels and are always considered as a positive integer. Because the noise matrix N is unknown, we substitute the least-squares estimate of the noise matrix $\|R_{\Omega} - \Omega \circ R\|_F^2$ for the first constraint in eq (6).

IV. PROPOSED ADMM-BASED CHANNEL ESTIMATION ALGORITHM

We addressed the constrained optimization task in eq (6) using the Lagrange duality method. The augmented Lagrangian of eq (6) is expressed as,

$$\begin{aligned} \mathcal{L}_A(Y, \bar{Z}, X, C, P_1, P_2) \triangleq & \Gamma_Y \|Y\|_* + \Gamma_{\bar{Z}} \|\bar{Z}\|_1 + \frac{1}{2} \|C\|_F^2 + \frac{1}{2} \|\Omega \circ \\ & X - R_{\Omega}\|_F^2 + \text{tr}(P_1^H(Y - X)) + \frac{\beta}{2} \|Y - X\|_F^2 + \text{tr}(P_2^H(C - \\ & X + A\bar{Z}B)) + \frac{\beta}{2} \|C - X + A\bar{Z}B\|_F^2, \end{aligned} \quad (7)$$

where, P_1, P_2 are dual variables (specify the size of these matrices) and $\beta > 0$ is the penalty parameter.

The symmetrical version of ADMM with a relaxation parameter is employed. This algorithm is different from the traditional ADMM [14] and it is based on Douglas–Rachford splitting method (DRSM) [21], [22]. The proposed ADMM is inspired from [23] where Fortin and Glowinski prove that attaching a relaxation parameter in ADMM leads to the faster convergence. The update rules of the proposed algorithm are given as,

$$Y^{(l+1)} = \underset{Y}{\text{argmin}} \mathcal{L}_A(Y, P_1^{(l)}, P_2^{(l)}, X^{(l)}, \bar{Z}^{(l)}, C^{(l)}), \quad (8a)$$

$$P_1^{(l+\frac{1}{2})} = P_1^{(l)} + \beta \mathcal{W}(X^{(l+1)} - Y^{(l)}), \quad (8b)$$

$$P_2^{(l+\frac{1}{2})} = P_2^{(l)} + \beta \mathcal{W}(C^{(l)} - X^{(l)} + A\bar{Z}^{(l)}B), \quad (8c)$$

$$X^{(l+1)} = \underset{X}{\text{argmin}} \mathcal{L}_A(Y^{(l+1)}, P_1^{(l+1)}, P_2^{(l+1)}, X, \bar{Z}^{(l)}, C^{(l)}), \quad (8d)$$

$$\bar{Z}^{(l+1)} = \underset{\bar{Z}}{\text{argmin}} \mathcal{L}_A(Y^{(l+1)}, P_1^{(l+1)}, P_2^{(l+1)}, X^{(l+1)}, \bar{Z}, C^{(l)}), \quad (8e)$$

$$C^{(l+1)} = \underset{C}{\text{argmin}} \mathcal{L}_A(Y^{(l+1)}, P_1^{(l+1)}, P_2^{(l+1)}, X^{(l+1)}, \bar{Z}^{(l+1)}, C), \quad (8f)$$

$$P_1^{(l+1)} = P_1^{(l+\frac{1}{2})} + \beta \mathcal{W}(X^{(l+1)} - Y^{(l+1)}), \quad (8g)$$

$$P_2^{(l+1)} = P_2^{(l+\frac{1}{2})} + \beta \mathcal{W}(C^{(l+1)} - X^{(l+1)} + A\bar{Z}^{(l+1)}B), \quad (8h)$$

where, all the variables are updated in symmetrical manner. \mathcal{W} is known as Fortin and Glowinski's relaxation parameter and the value of \mathcal{W} is fixed in between 0 and $\frac{1+\sqrt{5}}{2}$ [23].

Multiplication of relaxation parameter \mathcal{W} with the step size of ADMM can enlarge the step size and improve the convergence speed [24], [25].

The close form solution of $Y^{(l+1)}$ in eq (8a) can be obtained by the singular value thresholding (SVT) operation as [26],

$$Y^{(l+1)} = \text{Udiag}(\{\text{sign}(h_i) \max(h_i, 0)\}_{1 \leq i \leq r})V^H, \quad (9)$$

where, $U \in \mathbb{C}^{N_r \times r}$ and $V \in \mathbb{C}^{N_r \times r}$ are singular vector matrices of $(X^{(l)} - \frac{1}{\beta} P_1^{(l)})$. The SVT threshold operator Γ and r singular values are denoted by μ_i and $h_i \triangleq \mu_i - \frac{\Gamma}{\beta}$, respectively.

Also, subproblem in eq (8d) can be optimally tackled as,

$$X^{(l+1)} = (M^H M + 2\beta I_L)^{-1} (p_1^{(l)} + \beta y^{(l+1)} + M^H r_{\Omega} + p_2^{(l)} + \beta c^{(l)} + \beta O \bar{Z}^{(l)}), \quad (10)$$

where, I_L is the identity matrix, $M \triangleq \sum_{i=1}^{N_R} \text{diag}([\Omega]_k)^T \otimes E_{kk} [\Psi]_i$ exhibits the k -th row, and E_{kk} is derived by inserting unit values in the $N_R \times N_R$ zero matrix at its (k, k) -th position and $O \triangleq A_T^* \otimes A_R$.

Next, the optimal solution to subproblem in eq (8e) can be derived by the least absolute shrinkage and selection operator (LASSO) [27] as,

$$\begin{aligned} \bar{Z}^{(l+1)} = & \text{sign}\left(\text{Re}(v^{(l+1)})\right) \circ \max(|\text{Re}(v^{(l+1)})| - \Gamma'_{\bar{Z}}, 0) + \\ & \text{sign}\left(\text{Im}(v^{(l+1)})\right) \circ \max(|\text{Im}(v^{(l+1)})| - \Gamma'_{\bar{Z}}, 0), \end{aligned} \quad (11)$$

where, $\Gamma'_{\bar{Z}} \triangleq \frac{\Gamma_{\bar{Z}}}{\beta}$. $V^{(l+1)} = B^H A \left(\frac{1}{\beta} \left(\frac{1}{\beta} P_2^{(l+1)} - C^{(l)} + X^{(l+1)} \right) \right)$ is scaled version of $\Gamma_{\bar{Z}}$ and $v^{(l+1)} = \text{vec}(V^{(l+1)})$.

Finally, the close form solutions of $C^{(l+1)}$ to eq (8f) can be obtained as,

$$C^{(l+1)} = \frac{\beta}{\beta+1} \left(X^{(l+1)} - A\bar{Z}^{(l+1)}B + \frac{1}{\beta} P_2^{(l)} \right), \quad (12)$$

The optimal solutions of dual variable $P_1^{(l+1)}$ and $P_2^{(l+1)}$ can be derived with the help of primary and secondary variables.

V. SIMULATION RESULTS

This section assesses the proposed method via numerical results, For the simulations, we fix $N_T = 4$, $N_P = 6$, $L = 2$ and number of receive RF chains are set to $M_R = 24$ i.e., $L_R = 24$ is considered for the simulation. For the antenna deployment, we consider the uniform linear array (ULA) with 55° standard deviation to generate the AoAs and AoDs. Phase shifters with quantized phase have been used. The distance between antennas are set to be $d = \frac{\lambda}{2}$. The weighting factors have been considered at $\Gamma_Y = \frac{1}{\|R_Q\|}$ and $\Gamma_Z = \frac{1}{2\|Z\|}$. The step size β for the proposed approach is calculated as $\beta = \sqrt{\frac{\lambda_{\min} \Gamma_Y}{2}}$, where, λ_{\min} is the smallest eigenvalue of Y .

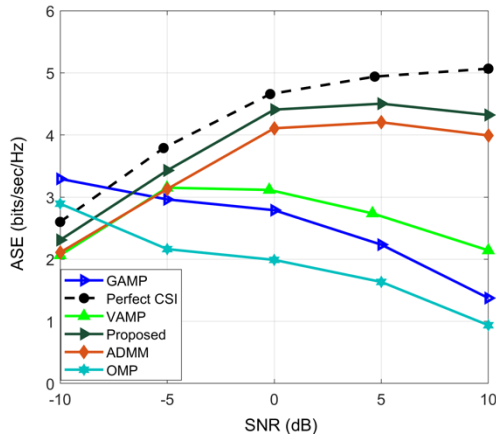


Fig. 2. Comparison of Average SE with respect to SNR.

Fig 2 represents the average SE performance with respect to signal-to-noise (SNR) ratio. For comparison, we consider four benchmark scheme, i.e., vector approximation message passing (VAMP) [28], generalized approximate message passing (GAMP)[[29], vanilla ADMM [14] and OMP [7]. The proposed algorithm performs well at -10 dB as compare to other benchmarks. As the SNR range is increasing the ASE performance of the proposed one is getting better. The considered channel is frequency selective. Hence, at +10 dB SNR, a slight downticking is noticed in the performance of proposed algorithm but still it outperformed the other benchmarks i.e., VAMP, GAMP, ADMM and OMP with respect to the perfect channel state information.

Fig. 3 compares the proposed algorithm with two-stage sparse representation (TSSR)[30], time domain orthogonal matching pursuit (TD-OMP)[9] and vanilla ADMM. In terms of normalised MSE defined as,

$$NMSE \triangleq E \left(10 \log_{10} \frac{\|\bar{Z} - \hat{Z}\|_F^2}{\|Z\|_F^2} \right).$$

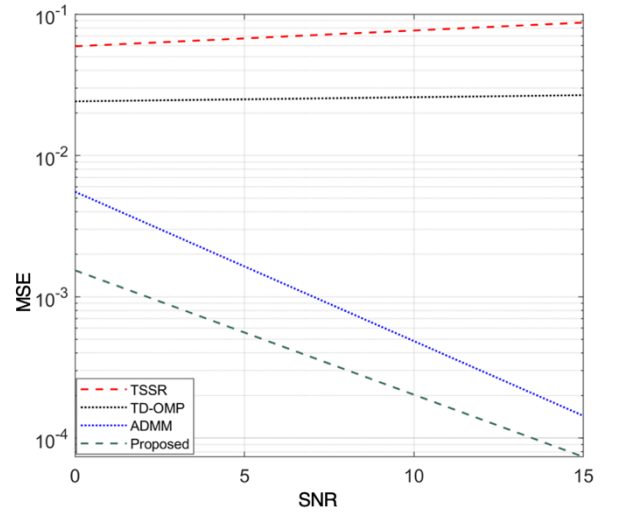


Fig. 3. Comparison of MSE with respect to SNR.

where \hat{Z} denotes the estimated channel matrix. The figure shows that the performance of the TD-OMP getting worst as the SNR level is increasing, and this is attributable to the vastness of its dictionary matrix. The TSSR uses two-stage estimation method which generally loses the optimality. On the other hand, the ADMM is a more flexible, which jointly exploits the low-rank and sparse properties of channel matrices, leading to the improved normalized MSE. The proposed algorithm is also like ADMM with larger step size. Therefore, the proposed algorithm outperformed all others at the considered SNR levels

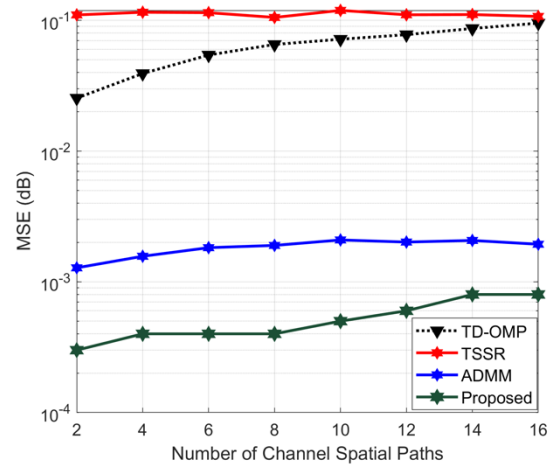


Fig. 4. Effect of no. of channel spatial path with respect to MSE.

The impact of the number of spatial paths on the estimation accuracy is investigated in. fig.4 which evaluates the normalized MSE in terms of N_p . As the number of channel spatial pathways grows, the performance of the TSSR and TD-OMP baselines. However, the ADMM and the proposed

algorithm performs better than any of the other benchmarks. For dependable communication, the NMSE of ADMM and the proposed algorithm are very substantial.

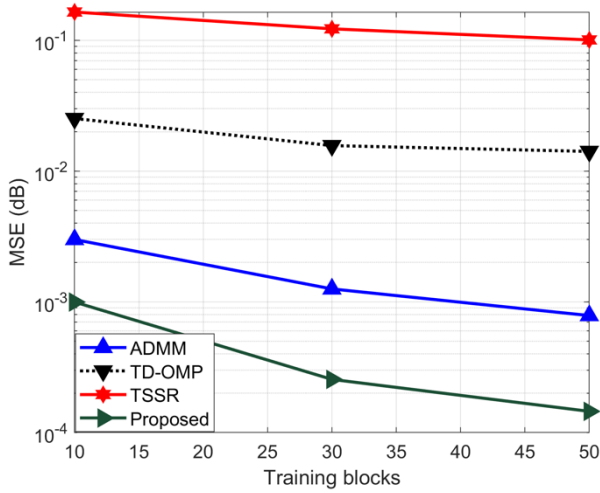


Fig. 5. Performance comparison of Training blocks with respect to MSE.

The MSE performance as a function of training blocks T is shown in fig. 5. The proposed method clearly outperforms other baseline schemes for all simulated training blocks. The normalized MSE of the proposed algorithm improves as the number of training blocks increases.

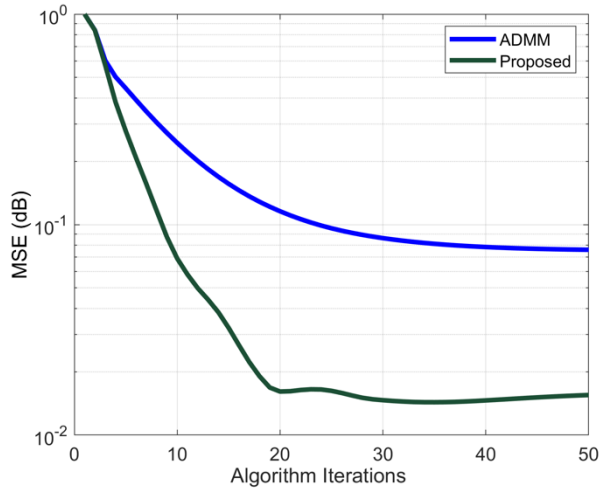


Fig. 6. Convergence analysis.

Fig. 6 exhibits the convergence behaviour of the proposed and ADMM algorithms. It is observed that proposed converges faster (less than 20 iterations) with better MSE performance as compared to the ADMM.

VI. CONCLUSION

This paper has proposed the ADMM-based channel estimation techniques for the frequency selective mmWave MIMO. The proposed algorithm exploits the low-rank and sparse structure of the dictionary matrix in a symmetrical order. The relaxation parameter increased the step size, resulting in a faster convergence. Simulation results have demonstrated the superiority of proposed methodology over several traditional and advance benchmarks.

ACKNOWLEDGEMENT

This work is supported by the National Research Foundation (NRF) of Korea grant funded by the Korea government Ministry of Science and ICT (MSIT) under the Grant No. 2021R111A3054575.

REFERENCES

- [1] H. Ji, S. Park, J. Yeo, Y. Kim, J. Lee, and B. Shim, "Ultra-reliable and low-latency communications in 5G downlink: Physical layer aspects," *IEEE Wirel. Commun.*, vol. 25, no. 3, pp. 124–130, 2018.
- [2] A. F. Molisch *et al.*, "Hybrid beamforming for massive MIMO: A survey," *IEEE Commun. Mag.*, vol. 55, no. 9, pp. 134–141, 2017.
- [3] R. W. Heath, N. Gonzalez-Prelcic, S. Rangan, W. Roh, and A. M. Sayeed, "An overview of signal processing techniques for millimeter wave MIMO systems," *IEEE J. Sel. Top. Signal Process.*, vol. 10, no. 3, pp. 436–453, 2016.
- [4] K. Venugopal, A. Alkhateeb, R. W. Heath, and N. G. Prelcic, "Time-domain channel estimation for wideband millimeter wave systems with hybrid architecture," in *2017 IEEE International Conference on Acoustics, Speech and Signal Processing (ICASSP)*, 2017, pp. 6493–6497.
- [5] A. Alkhateeb, O. El Ayach, G. Leus, and R. W. Heath, "Channel estimation and hybrid precoding for millimeter wave cellular systems," *IEEE J. Sel. Top. Signal Process.*, vol. 8, no. 5, pp. 831–846, 2014.
- [6] R. Méndez-Rial, C. Rusu, N. González-Prelcic, A. Alkhateeb, and R. W. Heath, "Hybrid MIMO Architectures for Millimeter Wave Communications: Phase Shifters or Switches?," *IEEE Access*, vol. 4, pp. 247–267, 2016, doi: 10.1109/ACCESS.2015.2514261.
- [7] J. Lee, G. Gil, and Y. H. Lee, "Channel Estimation via Orthogonal Matching Pursuit for Hybrid MIMO Systems in Millimeter Wave Communications," *IEEE Trans. Commun.*, vol. 64, no. 6, pp. 2370–2386, 2016, doi: 10.1109/TCOMM.2016.2557791.
- [8] G. C. Alexandropoulos and S. Chouvardas, "Low complexity channel estimation for millimeter wave systems with hybrid A/D antenna processing," in *2016 IEEE Globecom Workshops (GC Wkshps)*, 2016, pp. 1–6.
- [9] K. Venugopal, A. Alkhateeb, N. G. Prelcic, and R. W. Heath, "Channel estimation for hybrid architecture-based wideband millimeter wave systems," *IEEE J. Sel. Areas Commun.*, vol. 35, no. 9, pp. 1996–2009, 2017.
- [10] G. C. Alexandropoulos, "Position aided beam alignment for millimeter wave backhaul systems with large phased arrays," in *2017 IEEE 7th International Workshop on Computational Advances in Multi-Sensor Adaptive Processing (CAMSAP)*, 2017, pp. 1–5.
- [11] D. L. Donoho, "Compressed sensing," *IEEE Trans. Inf. theory*, vol. 52, no. 4, pp. 1289–1306, 2006.
- [12] T. T. Cai and L. Wang, "Orthogonal matching pursuit for sparse signal recovery with noise," *IEEE Trans. Inf. theory*, vol. 57, no. 7, pp. 4680–4688, 2011.
- [13] X. Li, J. Fang, H. Li, and P. Wang, "Millimeter wave channel estimation via exploiting joint sparse and low-rank structures," *IEEE Trans. Wirel. Commun.*, vol. 17, no. 2, pp. 1123–1133, 2017.
- [14] E. Vlachos, G. C. Alexandropoulos, and J. Thompson, "Massive MIMO Channel Estimation for Millimeter Wave Systems via Matrix Completion," *IEEE Signal Process. Lett.*, vol. 25, no. 11, pp. 1675–

1679, 2018, doi: 10.1109/LSP.2018.2870533.

- [15] D. Lee, S.-J. Kim, and G. B. Giannakis, "Channel gain cartography for cognitive radios leveraging low rank and sparsity," *IEEE Trans. Wirel. Commun.*, vol. 16, no. 9, pp. 5953–5966, 2017.
- [16] P. S. Srivastav, L. Chen, and A. H. Wahla, "Precise Channel Estimation Approach for a mmWave MIMO System," *Appl. Sci.*, vol. 10, no. 12, p. 4397, 2020.
- [17] F. Ma, M. Ni, X. Zhang, and Z. Yu, "Solving Lasso: Extended ADMM is more efficient than ADMM," in *2015 Chinese Automation Congress (CAC)*, 2015, pp. 55–58, doi: 10.1109/CAC.2015.7382469.
- [18] E. Vlachos, G. C. Alexandropoulos, and J. Thompson, "Wideband MIMO channel estimation for hybrid beamforming millimeter wave systems via random spatial sampling," *IEEE J. Sel. Top. Signal Process.*, vol. 13, no. 5, pp. 1136–1150, 2019.
- [19] J. Rodriguez-Fernandez and N. Gonzalez-Prelcic, "Channel Estimation for Frequency-Selective mmWave MIMO Systems with Beam-Squint," in *2018 IEEE Global Communications Conference (GLOBECOM)*, 2018, pp. 1–6, doi: 10.1109/GLOCOM.2018.8647269.
- [20] A. M. Sayeed, "Deconstructing multiantenna fading channels," *IEEE Trans. Signal Process.*, vol. 50, no. 10, pp. 2563–2579, 2002, doi: 10.1109/TSP.2002.803324.
- [21] J. Douglas and H. H. Rachford, "On the numerical solution of heat conduction problems in two and three space variables," *Trans. Am. Math. Soc.*, vol. 82, no. 2, pp. 421–439, 1956.
- [22] P.-L. Lions and B. Mercier, "Splitting algorithms for the sum of two nonlinear operators," *SIAM J. Numer. Anal.*, vol. 16, no. 6, pp. 964–979, 1979.
- [23] R. Glowinski, *Numerical methods for nonlinear variational problems*. Tata Institute of Fundamental Research, 1980.
- [24] C. Chen, B. He, and X. Yuan, "Matrix completion via an alternating direction method," *IMA J. Numer. Anal.*, vol. 32, no. 1, pp. 227–245, 2012.
- [25] B. He, M. Xu, and X. Yuan, "Solving large-scale least squares covariance matrix problems by alternating direction methods," *SIAM J. Matrix Anal. Appl.*, vol. 32, no. 1, p. 136, 2011.
- [26] J.-F. Cai, E. J. Candès, and Z. Shen, "A singular value thresholding algorithm for matrix completion," *SIAM J. Optim.*, vol. 20, no. 4, pp. 1956–1982, 2010.
- [27] R. Tibshirani, "Regression shrinkage and selection via the lasso," *J. R. Stat. Soc. Ser. B*, vol. 58, no. 1, pp. 267–288, 1996.
- [28] S. Rangan, P. Schniter, and A. K. Fletcher, "Vector approximate message passing," *IEEE Trans. Inf. Theory*, vol. 65, no. 10, pp. 6664–6684, 2019.
- [29] S. Rangan, "Generalized approximate message passing for estimation with random linear mixing," in *2011 IEEE International Symposium on Information Theory Proceedings*, 2011, pp. 2168–2172.
- [30] C. Peng, H. Cheng, and M. Ko, "An efficient two-stage sparse representation method," *Int. J. Pattern Recognit. Artif. Intell.*, vol. 30, no. 01, p. 1651001, 2016.